

# The Induced Magnetic Field in Cyclic Molecules

Gabriel Merino, Thomas Heine,\* and Gotthard Seifert<sup>[a]</sup>

**Abstract:** The response of a molecule to an applied external magnetic field can be evaluated by a graphical representation of the induced magnetic field. We have applied this technique to four representative, cyclic organic molecules, that is, to aromatic ( $C_6H_6$ ,  $D_{6h}$ ), anti-aromatic ( $C_4H_4$ ,  $D_{2h}$ ) and non-aromatic ( $C_4H_8$ ,  $D_{4h}$ , and  $C_6H_{12}$ ,  $D_{3d}$ ) molecules. The results show that molecules that contain a  $\pi$  system pos-

sess a long-range magnetic response, while the induced magnetic field is short-range for molecules without  $\pi$  systems. The induced magnetic field of aromatic molecules shields the external field. In contrast, the anti-aromatic

molecules increase the applied field inside the ring. Aromatic, anti-aromatic, and non-aromatic molecules can be characterized by the appearance of the magnetic response. We also show that the magnetic response is directly connected to nucleus-independent chemical shifts (NICS).

**Keywords:** aromaticity · carbocycles · induced magnetic field · magnetic properties

## Introduction

Few concepts are as frequently used as aromaticity in the current chemical literature.<sup>[1–5]</sup> The traditional criteria for aromaticity include chemical behavior (lower reactivity), structural features (planarity and equal bond length tendencies), energy (stability), and spectroscopic properties (UV, proton chemical shifts, magnetic susceptibility exaltation). More recently, several magnetic indices of aromaticity have been introduced and discussed.<sup>[6]</sup> They include nucleus-independent chemical shift (NICS)<sup>[7]</sup> and related indexes,<sup>[8–11]</sup> aromatic ring-current shielding (ARCS),<sup>[12]</sup> and plotted ring-current densities.<sup>[13,14]</sup> The most widely applied of these methods, NICS, is the negative shielding constant at a given position, typically at ring centers. As NICS is an easily accessible index and its interpretation is straightforward, it has been applied numerous times since its introduction in 1996.<sup>[11]</sup> However, its applicability is still discussed controversially in the scientific literature.<sup>[15]</sup>

In this work, we compute the induced magnetic field of a molecule in an external magnetic field. This induced field has been used by physicists to understand the magnetism of macroscopic physical objects (e.g., coils), but also by chem-

ists to understand the magnetic properties of molecules.<sup>[16,17]</sup> Related electrodynamic quantities, such as material constants, are accessible through the induced magnetic field and Maxwell's equations. The induced magnetic field ( $\mathbf{B}^{\text{ind}}$ ) at a position  $\mathbf{R}$  can be computed from the induced current density of the molecule ( $\mathbf{j}(\mathbf{r})$ ) by using Biot-Savart's law [Eq. (1)].

$$\mathbf{B}^{\text{ind}}(\mathbf{R}) = \frac{\mu_0}{4\pi} \int \frac{\mathbf{j}(\mathbf{r}) \times (\mathbf{r} - \mathbf{R})}{|\mathbf{r} - \mathbf{R}|^3} d\mathbf{r} \quad (1)$$

The NMR shielding tensor,  $\sigma$ , can be computed directly from this quantity.<sup>[18,19]</sup> Note that Equation (1) does not contain information about a nucleus, and, hence, the shielding tensor can be computed at any place in space; that is, at the position of a nucleus or somewhere else. The induced magnetic field  $\mathbf{B}^{\text{ind}}$  is related with the shielding tensor at position  $\mathbf{R}$  and the external magnetic field  $\mathbf{B}^{\text{ext}}$  [Eq. (2)].

$$\mathbf{B}^{\text{ind}}(\mathbf{R}) = -\sigma(\mathbf{R})\mathbf{B}^{\text{ext}} \quad (2)$$

As the shielding tensor can be computed by means of most recent quantum-chemistry programs at any level of theory, this approach is very practical for application.

In this first study, we restrict our analysis to four examples, which are characteristic cyclic molecules in organic chemistry: aromatic ( $C_6H_6$ ,  $D_{6h}$ ), anti-aromatic ( $C_4H_4$ ,  $D_{2h}$ ), and non-aromatic rings ( $C_4H_8$ ,  $D_{4h}$ , and  $C_6H_{12}$ ,  $D_{3d}$ ). The molecules are placed in such way that the ring is located in the  $xy$  plane with the center of the molecule in the origin of the coordinate system. The  $z$  axis is identical with the highest symmetry axis.

[a] Dr. G. Merino, Dr. T. Heine, Prof. Dr. G. Seifert  
Institut für Physikalische Chemie und Elektrochemie  
TU Dresden, 01062 Dresden (Germany)  
Fax: (+49)351-463-35953  
E-mail: thomas.heine@chemie.tu-dresden.de

Supporting information for this article is available on the WWW under <http://www.chemeurj.org/> or from the author.

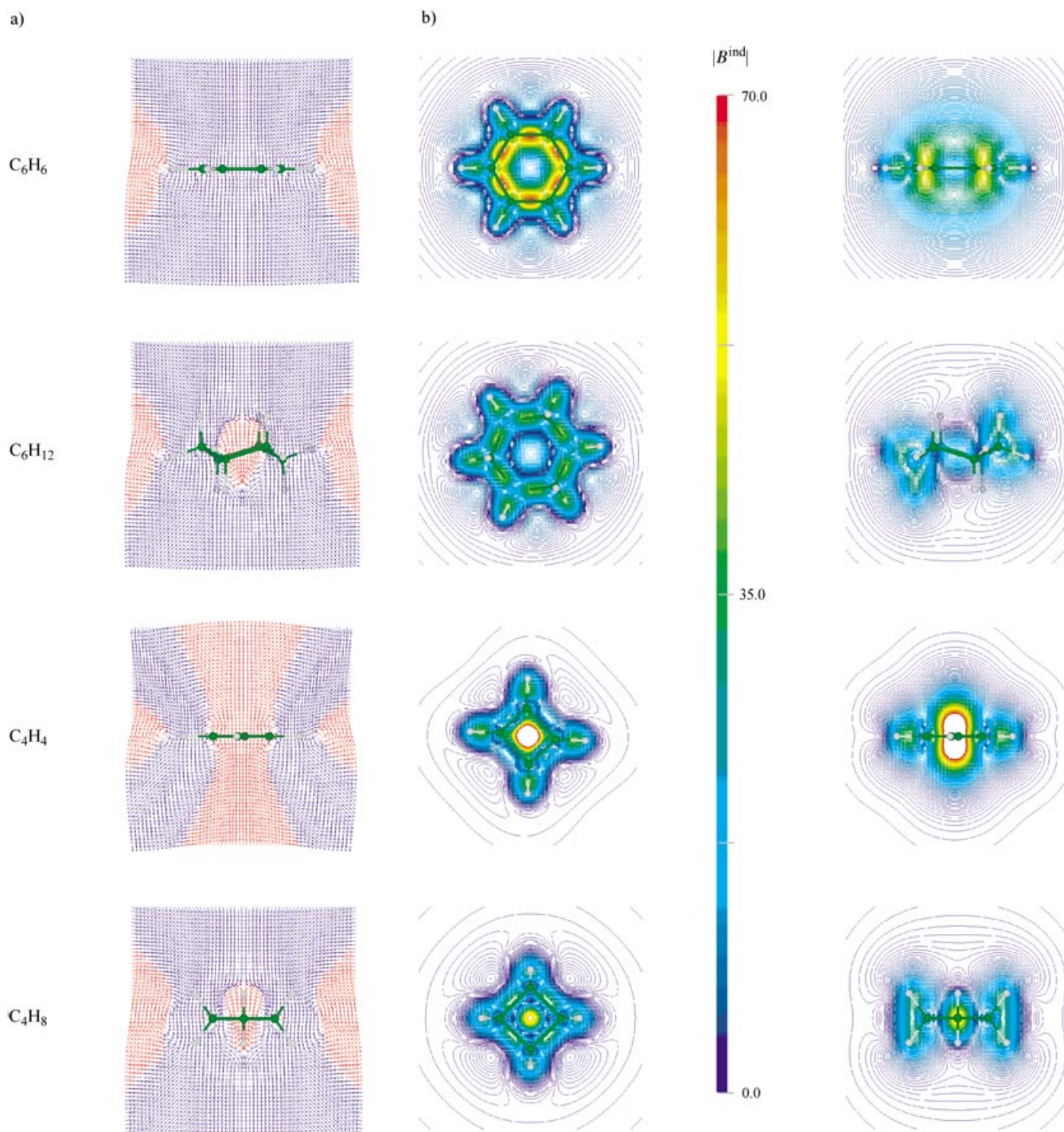


Figure 1. a) Induced magnetic fields of an external field in  $z$  direction to cyclic organic molecules located in the  $xy$  plane. Diatropic ( $B$  shielding) contributions are given in blue, paratropic contributions in red. Induced magnetic fields are in ppm, or, if the external field has the magnitude of 1 T, the unit of the induced field is  $\mu\text{T}$ . b) Magnetic field lines: contour lines of the magnitude  $|B^{\text{ind}}|$  of the external magnetic field perpendicular to the ring. The scale is given in ppm ( $\mu\text{T}$  for  $|B^{\text{ext}}| = 1 \text{ T}$ ). The plots are given in (center) and perpendicular to (right) the molecular plane through the origin.

## Computational Methods

All molecular structures have been fully optimized at the PW91/DZVP level<sup>[20,21]</sup> and found to be in very close agreement with the B3LYP/6-31G\* geometries used by the Schleyer group for several NMR studies.<sup>[7,9,10]</sup> The NMR calculations were performed using the PW91 functional and IGLO-III basis set.<sup>[22]</sup> Cartesian shielding tensors<sup>[23]</sup> were com-

puted applying the IGLO method,<sup>[24]</sup> which gave very similar results to other density functionals (see Table 1 in the Supporting Information) and to recent ab initio computations.<sup>[10]</sup> The deMon 2002 program<sup>[25]</sup> was used to compute the molecular orbitals, and the deMon-NMR package<sup>[26]</sup> for the shielding tensors. Induced magnetic fields were computed, by using Equation (2), from Cartesian shielding tensors, and are in ppm of the units of the external field. Assuming an external magnetic field of  $|B^{\text{ext}}|$

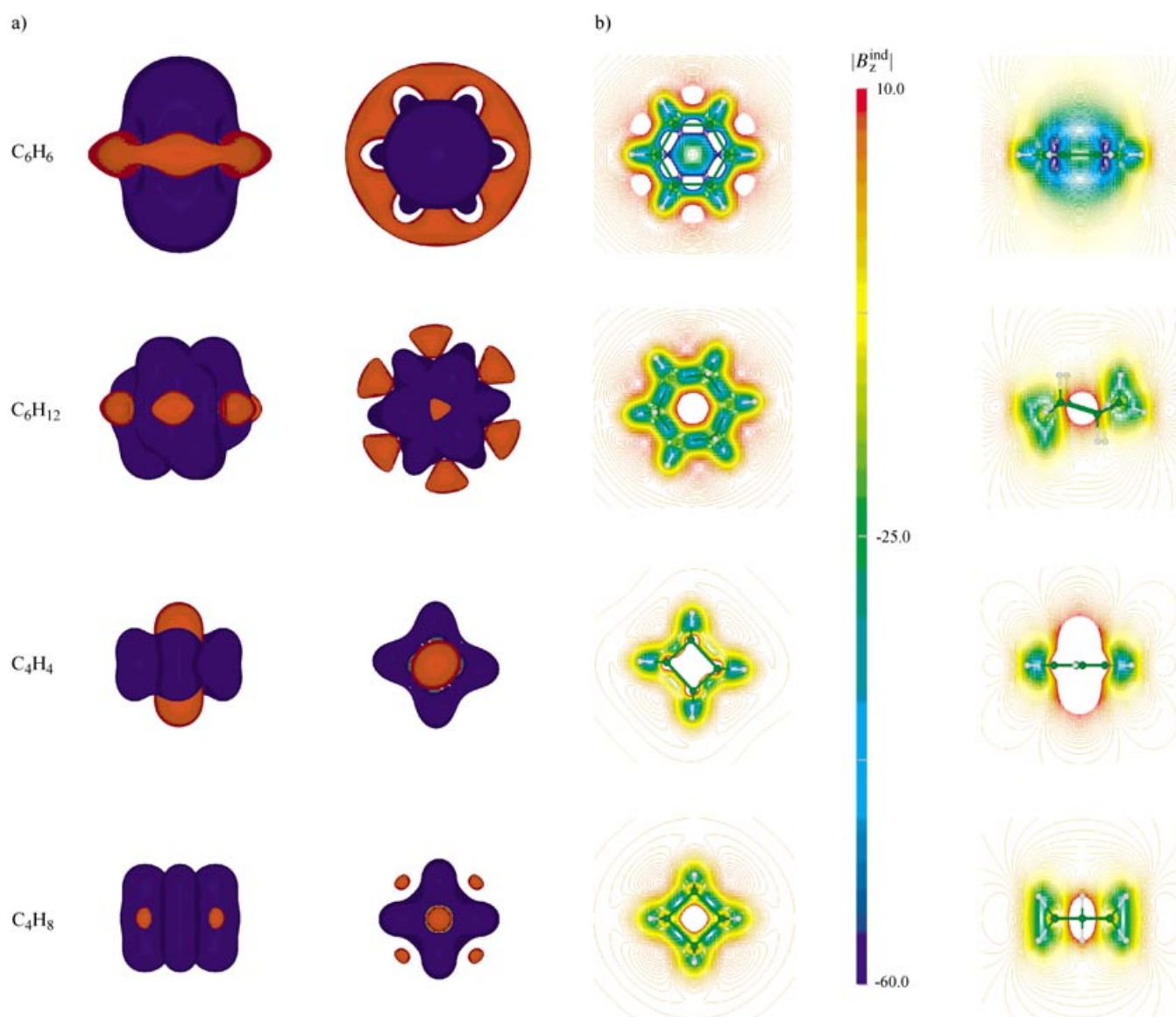


Figure 2. a) Isosurfaces of the z component of the induced magnetic field ( $B_z^{\text{ind}}$ ).  $|B_z^{\text{ind}}| = 4 \mu\text{T}$  and  $B^{\text{ext}} = 1 \text{ T}$  perpendicular to the molecular plane, given in top and front view of the molecule. Blue and red indicate shielding ( $|B_z^{\text{ind}}| < 0$ ) and deshielding areas, respectively. b) Contour lines of  $B_z^{\text{ind}}$  in the molecular plane and perpendicular to the molecular plane through the origin. The scale is given in ppm (or  $\mu\text{T}$  for an external field of 1 T).

$= 1 \text{ T}$ , the unit of the induced field is  $1 \mu\text{T}$ , which is equivalent to 1 ppm of the shielding tensor. VUJ<sup>[27]</sup> was employed for visualization of the induced field vectors as well as for their contour lines and isosurfaces. Cartesian shielding tensors of subsets of the computed grids, including the nuclei, are given in the Supporting Information.

## Results and Discussions

Figure 1 shows the induced magnetic fields of an external field applied perpendicular to the molecular planes. A magnetic field in this direction can induce a current density in and parallel to the molecular plane.<sup>[28–31]</sup> Following Equation (1), this current density induces a counter field, which is plotted in Figure 1. In this sense, the induced magnetic fields and induced current densities are complementary to each other. Induced current densities are usually given in

one selected plane parallel to the molecular ring, while the induced field contains information of the overall current density distribution. However, it is not clear whether the induced magnetic field originates from a ring current or not. Having both analyses available is therefore advantageous.

In agreement with current-density maps,<sup>[14,28,31]</sup> the response of our aromatic, anti-aromatic, and non-aromatic examples show characteristic features. In the aromatic example, benzene, no paratropic contributions are observed inside the ring. This is in contrast to the other three molecules and hence a direct consequence of the aromatic  $\pi$  system. Anti-aromatic  $C_4H_4$  shows a strong paratropic response inside and around the ring that is similar in magnitude and extension, but opposite in sign, to the diatropic response of benzene (see Figures 1 and 2). The non-aromatic molecules show a weakly paratropic response inside the rings. Around the  $\sigma$  framework, the interaction is always di-

atropic except for the anti-aromatic example. These trends are in agreement with the results of Schleyer et al., obtained by using NICS grids on top of the rings.<sup>[32]</sup>

Isosurfaces of the  $z$  component of the induced magnetic field,  $B_z^{\text{ind}}$ , with the external field perpendicular to the ring, are given in Figure 2a. For benzene, the shielding isosurface (given in blue) is around the molecule, while deshielding regions are further outside (given in red). For cyclobutadiene the situation is reversed. Figure 2a also shows that above and below the ring, the response of the molecule to the magnetic field is long-range for aromatic and anti-aromatic molecules (though different in sign), while the  $\sigma$  system is always surrounded by a diatropic region, independent if the system is aromatic, anti-aromatic, or non-aromatic. Hence, aromatic and anti-aromatic rings influence their surroundings through long-range magnetic fields; this can affect chemical shifts of surrounding nuclei, for example, in biological molecules and van der Waals crystals.<sup>[12,33]</sup> Note that  $B_z^{\text{ind}}$  for an external field perpendicular to the ring is equivalent to the  $zz$  or  $33$  component of the shielding tensor discussed earlier.<sup>[10]</sup> The  $x$  and  $y$  components of the induced magnetic field are given in Figure 1 in the Supporting Information. They have nodes in the ring plane and parallel to the  $z$  axis, and do not have as long a range as the  $B_z^{\text{ind}}$  component.

A particular observation for benzene is that the hydrogen atoms are located outside the vortexes of the induced field (see Figure 1) and inside the shielding rather than the deshielding region. A nodal ring, which separates the shielding from the deshielding region, encircles the molecule outside the hydrogen atoms (Figure 2a). This observation opposes popular text book explanations of abnormal  $^1\text{H}$  NMR chemical shifts of aromatic molecules, but is in agreement with related recent quantum chemical calculations of various groups.<sup>[34–37]</sup> However, the ring current model considers only ring currents arising from the  $\pi$  cloud, and our results also include the contributions from the  $\sigma$  framework.<sup>[38]</sup>

The response of benzene to an external magnetic field parallel to the molecular plane is of entirely different character than when the field is applied perpendicular to the ring; we observe short-range diatropic response parallel to the external field. Also for the other components, the response is limited to the region around the  $\sigma$  framework (see Figures 1 and 2 in the Supporting Information). Again, the hydrogen atoms are always in the shielding zone. Combining the results of all figures, we conclude that at long-range, the magnitude of the induced magnetic field is governed by its  $z$  component, or, in other words, to 1/3 of the negative NICS value if both quantities are given in ppm. Hence, the long-range contour plots become equivalent to the NICS grids computed by Schleyer et al.,<sup>[32]</sup> to iso-chemical shielding surfaces (ICSS) studied by Kleinpeter et al. earlier,<sup>[36,39]</sup> and to the aromatic ring-current shielding (ARCS) by Sundholm.<sup>[33]</sup>

Contour lines for the  $z$  component of the induced magnetic field ( $B_z^{\text{ind}}$ ) allow the quantification of the magnetic response. Figure 2b gives these contour lines for the four studied molecules, both on the molecular plane and on a plane perpendicular to the ring. Again, aromatic, anti-aromatic, and non-aromatic species show characteristic features in these plots. The aromatic molecule has a strongly shielding

region close to the carbons inside the ring (given in blue); this region has the form of the carbon  $\pi$  orbitals. Such features are not observed in any of the other molecules of this study. The anti-aromatic molecule shows a deshielding cone *outside* the ring, with the carbon atoms just inside the deshielding region. This detail cannot be observed by the isosurface plots of Figure 2a. The deshielding cone is very long-range and the shape of the carbon  $\pi$  orbitals cannot be seen in these plots. A shielding region is found around the C–H bond and around the hydrogen atoms. The non-aromatic systems again behave differently; a deshielding sphere is observed *inside* the rings, but the whole  $\sigma$ -framework, including the C–C bonds, is shielded. The contour lines again show that the response of non-aromatic molecules is short-ranged and relatively small. The largest response of all molecules studied here is observed for benzene in the area of the carbon  $\pi$  orbitals.

## Conclusions

We have shown that the simulation of the magnetic response of a molecule, represented by the induced magnetic field, is a meaningful analysis tool. Aromatic, anti-aromatic, and non-aromatic molecules show a characteristic response to an external field. The analysis allows the quantification of the (de)shielding area. According to present nomenclature, we suggest classifying molecules with long-range magnetic shielding as diatropic and those with long-range deshielding as paratropic.

The calculated induced magnetic fields, and the proper presentation of these vector fields as the linear response fields on an external magnetic field in molecules, gives unambiguous interpretations of the nuclear magnetic shielding and, hence, NMR data in molecules, as well as in solids in general. Furthermore, the induced magnetic field may serve as an, in principle, measurable quantity for characterization of the electronic structure of molecules and solids.

As  $B^{\text{ind}}$  contains contributions from  $\sigma$  and  $\pi$  electrons, their dissection is a next step for the development of the  $B^{\text{ind}}$  analysis. We also want to point out that the similar concept we introduce here could be applied to electric fields, which could give information about the electron polarization inside a molecule. Such investigations are currently in progress,<sup>[40]</sup> as are investigations on the magnetic response of several classes of molecules.

## Acknowledgements

The Deutsche Forschungsgemeinschaft (DFG) is thanked for financial support. We thank Clémence Corminboeuf for cheerful discussions.

- [1] V. I. Minkin, M. N. Glukhovtsev, B. I. F. A. Simkin, *Aromaticity and Anti-aromaticity: Electronic and Structural Aspects*, Wiley, New York, 1994.
- [2] P. von R. Schleyer, H. F. Jiao, *Pure Appl. Chem.* **1996**, *68*, 209.
- [3] D. Lloyd, *J. Chem. Inf. Comput. Sci.* **1996**, *36*, 442.
- [4] T. M. Krygowski, M. K. Cyranski, Z. Czarnocki, G. Hafelinger, A. R. Katritzky, *Tetrahedron* **2000**, *56*, 1783.

- [5] See special issue, *Chem. Rev.* **2001**, 101.
- [6] See special issue, *Phys. Chem. Chem. Phys.* **2004**, 6.
- [7] P. von R. Schleyer, C. Maerker, A. Dransfeld, H. F. Jiao, N. J. R. V. Hommes, *J. Am. Chem. Soc.* **1996**, 118, 6317.
- [8] P. von R. Schleyer, H. F. Jiao, N. J. R. V. Hommes, V. G. Malkin, O. Malkina, *J. Am. Chem. Soc.* **1997**, 119, 12669.
- [9] T. Heine, P. von R. Schleyer, C. Corminboeuf, G. Seifert, R. Reviakine, J. Weber, *J. Phys. Chem. A* **2003**, 107, 6470.
- [10] C. Corminboeuf, T. Heine, G. Seifert, P. von R. Schleyer, J. Weber, *Phys. Chem. Chem. Phys.* **2004**, 6, 273.
- [11] Z. Chen, T. Heine, P. von R. Schleyer, D. Sundholm, in *Calculation of NMR and EPR parameters. Theory and Applications*. (Eds.: M. Kaupp, M. Bühl, V. G. Malkin), Wiley-VCH, **2004**, p. 395.
- [12] J. Juselius, D. Sundholm, *Phys. Chem. Chem. Phys.* **1999**, 1, 3429.
- [13] S. Coriani, P. Lazzeretti, M. Malagoli, R. Zanasi, *Theor. Chim. Acta* **1994**, 89, 181.
- [14] P. W. Fowler, E. Steiner, R. Zanasi, B. Cadioli, *Mol. Phys.* **1999**, 96, 1099.
- [15] P. Lazzeretti, *Phys. Chem. Chem. Phys.* **2004**, 6, 217.
- [16] H. Günther, *NMR spectroscopy: Basic Principles, Concepts, and Applications in Chemistry*, 2nd ed., Wiley, Chichester, New York, **1995**.
- [17] K. Wolinski, *J. Chem. Phys.* **1997**, 106, 6061.
- [18] W. Bieger, G. Seifert, H. Eschrig, G. Grossmann, *Chem. Phys. Lett.* **1985**, 115, 275.
- [19] C. J. Jameson, A. D. Buckingham, *J. Chem. Phys.* **1980**, 73, 5684.
- [20] J. P. Perdew, Y. Wang, *Phys. Rev. B* **1992**, 45, 13244.
- [21] N. Godbout, D. R. Salahub, J. Andzelm, E. Wimmer, *Can. J. Chem.* **1992**, 70, 560.
- [22] W. Kutzelnigg, U. Fleischer, M. Schindler, *The IGLO-Method: Ab Initio Calculation and Interpretation of NMR Chemical Shifts and Magnetic Susceptibilities*, Vol. 23, Springer, Heidelberg, **1990**.
- [23] We wrote the Cartesian shielding tensor directly from the subroutine SIGOUT.f in deMon-NMR.
- [24] W. Kutzelnigg, *Isr. J. Chem.* **1980**, 19, 193.
- [25] A. M. Koster, G. Geudtner, A. Goursot, T. Heine, A. Vela, S. Patchkovskii, D. R. Salahub, NRC, Canada, **2002**.
- [26] V. G. Malkin, O. Malkina, D. R. Salahub, *Chem. Phys. Lett.* **1993**, 204, 80.
- [27] B. Ozell, R. Camarero, A. Garon, F. Guibault, *Finite Elem. Anal. Des.* **1995**, 19, 295.
- [28] P. Lazzeretti, *Prog. Nucl. Magn. Reson. Spectrosc.* **2000**, 36, 1.
- [29] R. W. A. Havenith, J. J. Engelberts, P. W. Fowler, E. Steiner, J. H. van Lenthe, P. Lazzeretti, *Phys. Chem. Chem. Phys.* **2004**, 6, 289.
- [30] E. Steiner, P. W. Fowler, *Int. J. Quantum Chem.* **1996**, 60, 609.
- [31] P. W. Fowler, E. Steiner, *J. Phys. Chem. A* **1997**, 101, 1409.
- [32] P. von Schleyer, M. Manoharan, Z. X. Wang, B. Kiran, H. J. Jiao, R. Puchta, N. Hommes, *Org. Lett.* **2001**, 3, 2465.
- [33] D. Sundholm, personal communication.
- [34] C. S. Wannere, P. von R. Schleyer, *Org. Lett.* **2003**, 5, 605.
- [35] E. Kleinpeter, S. Klod, *J. Am. Chem. Soc.* **2004**, 126, 2231.
- [36] S. Klod, E. Kleinpeter, *J. Chem. Soc. Perkin Trans. 2* **2001**, 1893.
- [37] M. O. Jensen, A. E. Hansen, *Adv. Quantum Chem.* **1999**, 35, 193.
- [38] J. A. Pople, *J. Chem. Phys.* **1956**, 24, 1111.
- [39] S. Klod, A. Koch, E. Kleinpeter, *J. Chem. Soc. Perkin Trans. 2* **2002**, 1506.
- [40] B. Gomez, A. Vela, personal communication.

Received: May 10, 2004  
Published online: August 5, 2004